Identification of Long Noncoding RNAs in Distinct Subtypes of Mouse Retinal Ganglion Cells

Ana Ayupe
University of Miami
Felipe Beckedorff
University of Miami
Konstantin Levay
University of Miami
Ramin Shiekhattar
University of Miami
Kevin Park (kpark@miami.edu)
University of Miami

Research Article

Keywords: Axon injury, retinal ganglion cell, axon regeneration, lncRNAs, retina, intrinsically photosensitive RGCs, direction selective RGCs, neuronal type specification, neuronal survival, neuronal apoptosis

Posted Date: January 25th, 2021

DOI: https://doi.org/10.21203/rs.3.rs-147625/v1

Identification of long noncoding RNAs in distinct subtypes of mouse retinal ganglion cells

Authors: Ana C. Ayupe[1*], Felipe Beckedorff[2], Konstantin Levay[1], Ramin Shiekhattar[2], Kevin K. Park[1*]

Affiliation:

[1]Miami Project to Cure Paralysis, Department of Neurosurgery, University of Miami Miller School of Medicine, 1095 NW 14th Ter. Miami, FL 33136

[2]University of Miami Miller School of Medicine, Sylvester Comprehensive Cancer Center, Department of Human Genetics, Biomedical Research Building, Room 719, 1501 NW 10th Avenue, Miami, FL 33136, USA

*Corresponding Authors: Kevin K. Park, kpark@miami.edu; Ana C. Ayupe, aca136@med.miami.edu

Abstract

Background: Emerging evidence indicates that long noncoding RNAs (lncRNAs) are important regulators of various biological processes, and their expression can be altered following certain pathological conditions, including central nervous system injury. Retinal ganglion cells (RGCs), whose axons form the optic nerve, are a heterogeneous population of neurons with more than 20 molecularly distinct subtypes. While most RGCs, including the ON-OFF direction-selective RGCs (ooDSGCs), are vulnerable to axonal injury, a small population of RGCs, including the intrinsically photosensitive RGCs (ipRGCs), are more resilient.

Results: By performing systematic analyses on RNA-sequencing data, here we identify lncRNAs that are expressed in ooDSGCs and ipRGCs with and without axonal injury. Our results reveal a repertoire of different classes of lncRNAs, including long intergenic noncoding RNAs and antisense ncRNAs that are differentially expressed between these RGC types. Strikingly, we also found dozens of lncRNAs whose expressions are altered markedly in response to axonal injury, some of which are expressed exclusively in either one of the subtypes. Moreover, analyses into these lncRNAs unraveled their neighboring coding genes, many of which encode transcription factors and signaling molecules, suggesting that these lncRNAs may act *in cis* to regulate important biological processes in these neurons. Lastly, guilt-by-association analysis showed that lncRNAs are correlated with apoptosis associated genes, suggesting potential roles for these lncRNAs in RGC survival.

Conclusions: Overall, the results of this study reveal RGC type-specific expression of lncRNAs and provide a foundation for future investigation of the function of lncRNAs in regulating neuronal type specification and survival.

Keywords

Axon injury, retinal ganglion cell, axon regeneration, lncRNAs, retina, intrinsically photosensitive RGCs, direction selective RGCs, neuronal type specification, neuronal survival, neuronal apoptosis.

Background

Long noncoding RNAs (lncRNA) have been shown play vital roles in regulating gene expression networks in developmental, physiological, and pathological processes. LncRNAs are a diverse class of transcribed RNAs, defined as transcripts with lengths exceeding 200 nucleotides that do not encode proteins. Broadly, lncRNAs are classified into four types: i) long intergenic noncoding RNAs (lincRNA) transcribed from intergenic regions; ii) intronic lncRNAs, transcribed entirely from introns of protein-coding genes; iii) sense lncRNAs, transcribed from the sense strand of protein-coding genes, and iv) antisense lncRNAs (AS lncRNAs), transcribed from the antisense strand of protein-coding genes. The majority (~78%) of lncRNAs are exemplified as tissue-specific, as opposed to only ~19% of mRNAs (1). In addition, lncRNAs are characterized by higher developmental stage- and cell type-specificity in the central nervous system (CNS) than the mRNA counterparts (2).

Retinal ganglion cells (RGCs), which are the sole output neurons in the retina, send projections to the brain, and convey visual information. During the early developmental stage, a combination of transcription factors determine the fate of RGCs (3-6). Remarkably, despite general features, RGCs also acquire subtype-specific characteristics that are strictly related to particular functions. In fact, there are more than 20 different subtypes of RGCs in the mouse, most of which are

molecularly and physiologically distinct from each other. However, the molecular mechanisms by which different RGC subtypes are specified during development remain unclear.

Another prominent feature of RGCs is the subtype-specific differences in their response to an injury. Studies have demonstrated that several subclasses of alpha RGCs and intrinsically photosensitive RGCs (ipRGCs) are particularly resilient, whereas most direction selective-RGCs (DSGCs) are vulnerable to axonal injury (7-12). Although several studies have described distinct transcription factors and signaling molecules that might contribute to the differential responses of injured RGCs, our understanding of the underlying mechanisms remain fragmentary.

To investigate the molecular mechanisms underlying the exceptional survival and regenerative ability of ipRGCs after axonal injury, we previously performed RNA-sequencing (RNA-seq) on these RGCs and the vulnerable RGC subtype, ON-OFF direction-selective RGCs (ooDSGCs) (7). Subsequently, we had reported hundreds of coding genes that were uniquely expressed in these RGC subtypes with and without optic nerve crush injury. In addition to our study, others have reported expression profiles of coding genes that were differentially expressed between various RGC subtypes (13, 14). However, subtype-specific expression of lncRNAs in RGCs has not been systematically examined. In this study, we analyze RNA-seq data from purified murine RGCs and identify lncRNAs that are expressed in two contrasting RGC subtypes (i.e. injury-resilient ipRGCs and the injury-vulnerable ooDSGCs) in normal and optic nerve-injured animals.

Methods

Identification of lncRNAs by analyzing the RNA-seq data

RNA-seq data obtained from isolated ipRGCs and ooDSGCs of optic nerve axotomized (i.e. 3 days post crush) and normal (i.e. sham surgery) mice (7) were used for the lncRNA analyses. RNA-seq data were previously deposited under the accession number GEO: GSE115661 (7). For the analyses in this current study, trimmed reads were aligned to the mm10 version of the mouse genome with STAR (15), followed by an assembly using the Cufflinks 2.2 tool. For the alignment and assembly we used GTF file from GENCODE version M17 (vM17; release 04/2018).

To classify the transcripts as putative novel lincRNAs, we used the method described in (16) with some modifications. Briefly, all reads that overlapped or were in a window of ±2 kb of the known mouse GENCODE genes were removed. Next, we generated transcriptome assemblies using Cufflinks 2.2 (17) for each of these samples separately and then used Cuffmerge to combine all annotations. All transcripts that were identified in these analyses as class code 'u' by Cuffmerge (class code "u" – putative novel intergenic transcripts) were retained. Transcripts with length < 200 nt and/or monoexonic transcripts were removed. Additionally, all transcripts with coding potential, as assessed by the Coding Potential Calculator (CPC version 2) (18) were discarded, resulting in a set of novel lincRNAs. This set was then combined with the mouse GENCODE vM17 transcripts, generating a list of lncRNAs (antisense lncRNAs and lincRNAs from GENCODE and novel lincRNAs identified in this work) that are expressed in ipRGCs and ooDSGCs.

Differential expression analysis

The RNA abundance defined as the FPKM (Fragments Per Kilobase Million) and the sum of exon read count per gene was calculated using RSEM (19), and differential expression (DE) analysis was performed with DESeq2. A gene was considered detected if the FPKM was > 0.3 in

at least two replicates of one sample and significantly changed if the adjusted p-value was < 0.05.

Gene ontology (GO) enrichment analysis

We used DAVID v6.8 to perform GO enrichment analysis (20). "Biological Process" and "Molecular Function" GO terms with p-value < 0.05 were defined as enriched.

Nearest-neighbor gene analysis of lncRNA

Protein-coding genes within 300 kb upstream or downstream of differentially expressed (DE) lncRNA locus were considered as lncRNA neighbors and its putative *cis*-targets. This analysis was performed separately for each dataset of DE lncRNAs; injured ipRGCs vs. normal ipRGCs; injured ooDSGCs vs. normal ooDSGCs; injured ooDSGCs vs. injured ipRGCs; normal ooDSGCs vs. normal ipRGCs. When both mRNA neighbors (upstream and downstream) were located at a distance less than 300 kb from the lncRNA, but only one of them was DE, we selected the DE as the lncRNA neighbor. When both neighbors were non-DE, we selected the closest mRNA as the lncRNA neighbor. Next, we searched for enriched "Biological Process" and "Molecular Function" Gene Ontology terms among each set of lncRNA-nearby mRNAs (see above).

Gene expression correlation analysis of lncRNA and mRNA

To predict the potential role of lncRNAs, we performed guilt-by-association analysis (21). Pearson correlation values of FPKM expression profiles were calculated for each lncRNA to all mRNAs across the four RGC groups. We constructed Pearson correlation matrices including the DE mRNAs and the DE lncRNA in the following RGC group comparisons: injured ipRGCs vs. normal ipRGCs; injured ooDSGCs vs. normal ooDSGCs; injured ooDSGCs vs. injured ipRGCs;

and normal ooDSGCs vs. normal ipRGCs. For each lncRNA, we considered its correlated protein-coding mRNAs, transcripts with a cutoff at Pearson correlation coefficient of $-0.9 > r > 0.9$. Gene Ontology enrichment analysis of mRNAs correlated with lncRNAs was performed separately for each DE comparison, except for the injured ipRGCs vs. normal ipRGCs, since we did not find any correlated lncRNA- mRNA pairs in this set of DE transcripts. For each DE comparison, we used the mRNAs in the correlation lncRNA-mRNA clusters for performing the GO analysis (see above).

Animals

C57BL6/J and B6.Cg-Tg(Thy1-CFP)23Jrs/J (hereafter referred as Thy1-CFP) mice between 9 - 11 weeks of age were used in this study. All experimental procedures were performed in compliance with protocols approved by the Institutional Animal Care and Use Committee (IACUC) at University of Miami (Permit Number: 19-150). For optic nerve crush, mice were anaesthetized with isoflurane, and buprenorphine (0.05 mg/kg) was administrated as post-operative analgesic. This study was carried out in compliance with the Animal Research: Reporting of In Vivo Experiments (ARRIVE) guidelines.

Optic nerve crush

For the injury procedure, the left optic nerve was exposed intraorbitally and crushed with jeweler's forceps (Dumont #5, Roboz) for 10 seconds approximately 1 mm behind the optic disc.

Tissue preparation and immunohistochemistry

Thy1-CFP mice were perfused transcardially with PBS followed by 4% paraformaldehyde (PFA) in PBS, then eyes were dissected and postfixed with 4% PFA in PBS overnight at 4°C. Samples were cryoprotected by incubating in 30% sucrose in PBS for 48 hours. Eyes were cryosectioned

to 16-µm thickness. Tissue sections were blocked in 5% normal donkey serum and 0.3% Triton X-100 in PBS for 1 hour and incubated with primary antibodies diluted in blocking buffer overnight at 4°C, followed by 1-hour incubation with secondary antibodies at room temperature. Primary antibodies used were rabbit anti-RBPMS 1:200 (PhosphoSolutions; cat# 1830) and chicken anti-GFP 1:1000 (Abcam; cat#13970).

Retinal ganglion cell purification

Three days after optic nerve crush, retinas were dissociated using papain digestion (17 U/ ml papain, Worthington; 5.5 mM L-cysteine; 0.006% DNase; 1.1 mM EDTA in DMEM/2% B27) during 30 minutes at 37°C as previously described at (1). After digestion, retinas were washed in DMEM, gently triturated using a Pasteur pipet and centrifuged at 300 g x 5 min at RT. Dissociated cells were resuspended in DMEM/2% B27, passed through a 35 µm cell strainer and placed on ice until use. Dissociated retinal cells were stained with Ghost red 780 (TONBO Biosciences) to exclude non-viable cells and then CFP cells were separated by BD FACS SORP Aria-IIu (BD Biosciences) at Flow Cytometry Shared Resource, University of Miami, Sylvester Comprehensive Cancer Center. C57BL6/J retinal cells were used as unstained control. Sorted cells were collected in PBS and immediately frozen at -80°C.

Reverse transcription and quantitative real-time PCR (RT-qPCR)

We validated the expression of one randomly selected novel lincRNA (XLOC_034401) in purified RGCs using RT-PCR. To validate RGC purification (Figure S3B and S3C), total RNA of FACS isolated RGCs from Thy1-CFP mice was extracted using RNeasy Micro Kit (Qiagen) and treated with DNase I according to the manufacturer's instructions. 500 pg of total RNA was poly(A) amplified and reverse transcribed with MessageBOOSTER™ cDNA Synthesis Kit for

qPCR (Lucigen). Quantitative real-time PCR was performed to measure specific genes used as controls (*Thy1* and *Slc17a6* as markers for RGCs, and *Rho* as a marker for rods) using PowerUp™ SYBR® Green Master Mix (Applied Biosystems) on a QuantStudio 3 (Applied Biosystems). *Hprt* (hypoxanthine guanine phosphoribosyl transferase) was used as the endogenous control. PCR product was analyzed by Sanger sequencing at GENEWIZ. The primers used are listed in Additional file 1: Table S1.

Results

Identification of lncRNAs in ipRGCs and ooDSGCs

To identify the repertoire of lncRNAs that are expressed in ipRGCs and ooDSGCs, we analyzed the RNA-seq data obtained from isolated murine ipRGCs and ooDSGCs (7). In addition to the normal uninjured condition, we examined lncRNA expression of these RGC types extracted three days after intraorbital optic nerve crush (7). Thus, we analyzed a total of four RGC groups: normal ipRGCs, injured ipRGCs, normal ooDSGCs and injured ooDSGCs.

RNA-seq reads were aligned to the genome and assembled using a reference transcriptome that includes the lncRNAs from the mouse GENCODE vM17 with novel lncRNAs identified in this work (Fig. 1a). This generated a catalog of the lncRNAs, including antisense lncRNAs and lincRNAs that are expressed in ipRGCs and ooDSGCs (Additional file 2: Table S2).

We identified 639 and 547 lncRNAs in normal and injured ipRGCs, respectively (Fig. 1b). For ooDSGCs, we found 811 and 790 lncRNAs in normal and injured groups, respectively (Fig. 1b). Overall, we detected a total of 1,342 lncRNAs (Fig. 1b), of which 270 (20%) were identified as putative novel lincRNAs (i.e. not present in the GENCODE vM17) expressed in at least one of

197 the four RGC groups (Additional file 8: Fig. S1c). We detected 94 (15%) and 72 (13%) novel
198 lincRNAs in normal and injured ipRGCs, respectively (Additional file 8: Fig. S1c). Similarly, we
199 detected 138 (17%) and 136 (17%) novel lincRNAs in normal and injured ooDSGCs,
200 respectively (Additional file 8: Fig. S1c).

201 Next, we compared lncRNA expression profiles with those of the protein-coding mRNAs. For
202 lncRNAs, 32% (264/827) and 48% (515/1,078) were detected exclusively in ipRGCs and
203 ooDSGCs (Fig. 1b), respectively; in contrast, for the mRNAs, only 5% (605/12,228) and 9%
204 (1,138/12,761) were detected exclusively in ipRGCs and ooDSGCs, respectively (Fig. 1c). These
205 data indicate a higher RGC type-specific expression for lncRNAs compared to mRNAs (chi-
206 square test; $p < 0.0001$). We also examined injury-specific lncRNAs for each RGC type. Of all
207 the lncRNAs detected in ipRGCs (i.e. both normal and injured conditions), 34% (280/827) were
208 detected exclusively in normal, and 23% (188/827) in injured condition. In contrast, for the
209 mRNAs, only 7% (894/12,228) were expressed exclusively in normal, and 4% (527/12,228) in
210 injured condition (differences between lncRNAs and mRNAs for normal and injured conditions
211 were statistically significant; chi-square test; $p < 0.0001$). A similar pattern was seen for
212 ooDSGCs. In ooDSGCs, 27% of lncRNA were detected exclusively in normal (288/1,078), and
213 25% (267/1,078) in injured condition. On the other hand, for the protein coding genes, only 4%
214 (504/12,761) and 7% (856/12,761) of the transcripts were detected exclusively in normal and
215 injured condition, respectively (differences between lncRNAs and mRNAs for normal and
216 injured conditions were statistically significant; chi-square test; $p < 0.0001$).

217 Next, we compared our lincRNA data, including novel lincRNAs, to the lincRNA data from
218 whole retina RNA-seq (22). Reflecting the fact that ipRGCs and ooDSGCs represent only a
219 small fraction of the total retinal cells (23), we found that only 15% (54/363) of lincRNAs,

including novel lincRNAs, identified in normal ipRGCs were also identified in the whole retina RNA-seq (22) (Additional file 3: Table S3). For normal ooDSGCs, we found that 12% (58/467) of lincRNAs were also seen in the whole retina RNA-seq (Additional file 3: Table S3). Of the lincRNAs seen in the whole retina RNA-seq (272 transcripts, with a minimum FPKM > 0.3), 24% (64/272) were also detected in at least one of the two RGC subtypes. Among these 64 transcripts, 64% (41/64) were detected in both RGC types, suggesting they may represent broadly expressed lncRNAs.

General characteristics of lncRNAs expressed in ipRGCs and ooDSGCs

To further examine lncRNAs transcribed in ipRGCs and ooDSGCs, we subdivided them according to their genomic location in relation to the protein coding genes. Antisense lncRNAs are transcribed from the opposite strand of the protein coding genes, whereas lincRNAs are located between protein coding genes. The numbers of antisense lncRNAs, lincRNAs, and novel lincRNAs detected for each condition are shown in Additional file 2: Table S2 and Additional file 8: Fig. S1. In line with the previous studies (1, 24), we observed that lncRNAs have lower abundance compared to protein-coding genes (Fig. 2) (t-test; p-value < 0.001). For lncRNAs, the median FPKM for normal and injured ipRGCs were 2.3 and 2.6, respectively (Fig. 2a and 2b). For mRNAs, the median FPKM for normal and injured ipRGCs were 15 and 16.2, respectively. For ooDSGC lncRNAs, the median FPKM for normal and injured conditions were 1.6 and 1.8, respectively. The medians of mRNA for normal and injured ooDSGCs, were 13.1 and 13.7, respectively (Fig. 2c and 2d). Additionally, we compared the median FPKM for lncRNAs detected in RGCs with the median FPKM for lincRNAs detected in the whole retina RNA-seq (median FPKM = 1.5; Additional file 8: Fig. S2a and S2b) (22). However, we did not find a statistically significant difference from this comparison.

We found that the average length of lncRNAs for ipRGCs and ooDSGCs were 1.62 kb and 1.57 kb, respectively (Fig. 3a). On average, lncRNAs were shorter than mRNAs in length (t-test, p-value < 0.001; Fig. 3a). Moreover, lncRNAs were less spliced, with an average of 2.7 exons per transcript; whereas the average for protein-coding genes was 8.6 exons per transcript (t-test, p-value < 0.001; Fig. 3b). Compared to the whole retina lincRNAs, the average length of RGC lncRNAs was shorter (t-test, p-value < 0.001; Additional file 8: Fig. S2c). Similarly, the average number of exons in RGCs was smaller compared to that of the whole retina lincRNAs (t-test, p-value < 0.001; Additional file 8: Fig. S2d).

LncRNAs differentially expressed in ipRGCs and ooDSGCs

Since very little is known about lncRNAs that are expressed in different RGC types, we sought to identify differentially-expressed lncRNAs in ipRGCs and ooDSGCs. We detected 8 lncRNAs that were differentially expressed (adj p-value < 0.05) between normal and injured ipRGC groups, and 81 lncRNAs differentially expressed between normal and injured ooDSGC groups (Fig. 4a and 4b). Only 1 putative novel lincRNA was differentially expressed between normal and injured ipRGCs, whereas 21 putative novel lincRNAs were differentially expressed between normal and injured ooDSGCs. Thus, although the amount of lncRNAs expressed in these RGC types is similar (827 transcripts in ipRGCs and 1,078 in ooDSGCs; Fig. 1b), the number of lncRNAs whose expression is significantly altered by injury is markedly lower in ipRGCs compared to ooDSGCs (Fig. 4a and 4b).

Next, we sought to identify lncRNAs that are differentially expressed between injured ooDSGCs and injured ipRGCs as well as those that are differentially expressed between normal ooDSGCs and normal ipRGCs. For the injury group comparison, we detected 103 lncRNAs that were differentially expressed, whereas for the normal group comparison, we identified 112

differentially-expressed lncRNAs (Fig. 4c and 4d). Of these lncRNAs, 28 and 35 correspond to putative novel lincRNAs for each comparison, respectively. A full list of the differentially-expressed lncRNAs is provided in Additional file 4: Table S4. We validated the expression of one randomly selected novel lincRNA using RT-PCR (Additional file 8: Fig. S3).

Functional annotation of lncRNA-nearby protein-coding mRNA

Several studies have shown that lncRNAs can regulate their neighboring genes in a *cis*-acting manner. These *cis*-acting lncRNAs constitute a sizeable fraction of lncRNAs, and regulate gene expression in a manner dependent on the location of their own sites of transcription, at varying distances from their targets (25). To probe the potential roles of lncRNAs identified in RGCs, we examined protein-coding genes transcribed within 300 kb (upstream or downstream) of lncRNA loci. Using this criterion, we identified 610 nearby protein-coding genes in normal ipRGCs, 525 in injured ipRGCs, 777 in normal ooDSGCs, and 755 in injured ooDSGCs. Additional file 2: Table S2 contains a full list of these genes.

Notably, among the neighboring genes, we found protein-coding genes whose protein products are known to regulate cell death and apoptosis. For example, nearest-neighbor analysis identified *Ecel1*, a known injury-induced gene, as the closest neighbor of the lincRNA *RP23-416O18.4* (Gm29374). Our data showed that this lncRNA is one of the most highly upregulated lncRNAs in ooDSGCs after axonal injury. Similarly, our RNA-seq showed that *Ecel1* mRNA expression is highly induced in ooDSGCs after axonal injury, to an extent far greater than the level seen in ipRGCs; *Ecel1* mRNA FKPM for injured ooDSGCs is 384 and for injured ipRGCs is 37. *Ecel1* was not detected in normal ooDSGCs and normal ipRGCs (7).

To systematically deduce the biological functions of lncRNAs based on the functions of their nearby mRNAs (i.e. potential *cis*-targets), we performed Gene Ontology (GO) enrichment analysis on the protein-coding genes neighboring the differentially-expressed lncRNAs. Results from this analysis are described below. The level of gene expression for the protein-coding mRNAs that are neighbors of the differentially-expressed lncRNAs are shown in Additional file 8: Fig. S4-S6.

Nearby protein-coding genes of lncRNAs that were differentially expressed between injured and normal ipRGCs

"Zinc ion binding" was the only GO term significantly enriched in this group comparison because of the small number of differentially-expressed lncRNAs. One of the nearby genes enriched to this term is *Shank3* (Fig. 5a, Additional file 5: Table S5), which encodes for a synaptic scaffolding protein that is associated with neurodevelopmental disorders (26).

Nearby protein-coding genes of lncRNAs differentially expressed between injured and normal ooDSGCs

Significantly enriched GO categories in this group comparison include "positive regulation of cyclic-nucleotide phosphodiesterase activity", "metal ion binding", "cell adhesion molecule binding", "heterophilic cell-cell adhesion via plasma membrane cell adhesion molecules", and "adenylate cyclase binding" (Fig. 5b, Additional file 5: Table S5).

Nearby protein-coding genes of lncRNAs differentially expressed between injured ooDSGCs and injured ipRGCs

Most of the significantly enriched GO terms in this group comparison were those that are associated with transcription, development, and axon growth, including "transcription factor

activity sequence-specific DNA binding", "neuron migration", "nervous system development" "miRNA binding", "forebrain development", "embryonic skeletal system morphogenesis" and "axonogenesis" (Fig. 5c, Additional file 5: Table S5).

Nearby protein-coding genes of lncRNAs differentially expressed between normal ooDSGCs and normal ipRGCs

Similar to the terms listed above, significantly enriched GO terms in this group comparison include "neuron migration", "regulation of axon extension" "nervous system development" and "transcription factor activity sequence-specific DNA binding" (Fig. 5d, Additional file 5: Table S5). Notably, among the genes enriched in the term "regulation of transcription", there are several transcription factors that are known to be expressed specifically in these two RGC types. For example, *Eomes* (also known as *Tbr2*) was identified in our analysis as a neighbor of lncRNAs detected exclusively in ipRGCs (Additional file 2: Table S2). *Eomes* knockout was shown previously to cause death of ipRGCs in uninjured mice (4) as well as in mice with optic nerve crush (7), demonstrating that *Eomes* is essential to the survival of ipRGCs.

Additionally, we identified *Pou4f1* (also known as *Brn3a*) and *Pou4f3* (also known as *Brn3c*) as neighbors of lncRNAs that were detected exclusively in ooDSGCs. The Brn3/Pou4f transcription factors are known to participate in RGC development and type specification (5, 27). We and others have previously shown that ooDSGCs, but not ipRGCs, exhibit high levels of *Brn3a* and *Brn3c* expression (7, 14, 28), raising the possibility that these lncRNAs may play functional roles in regulating expression of these genes and promoting RGC type specification.

Functional annotation of gene-lncRNA co-expression networks

Many lncRNAs do not have a known biological function. Therefore, we performed guilt-by-association analysis (21) to predict the putative roles of the RGC lncRNAs seen in our study. Pearson correlation values of FPKM expression profiles were calculated for each lncRNA to all mRNAs across the four RGC groups. We identified potential associations based on Pearson correlated coefficient ($r > |0.9|$) for the differentially-expressed lncRNAs and mRNAs (Figs. 6 and 7). Only the transcripts (i.e. lncRNAs and mRNAs) detected in all four RGC groups were used in this analysis. Each lncRNA shown in Figure 6a and Figure 7 was correlated with at least one protein-coding gene (Additional file 6: Table S6). We grouped the protein-coding genes in correlation clusters, based on their positive or negative correlation with the lncRNAs. Then, we used GO enrichment analysis to infer functions for the lncRNAs correlated with mRNAs within each specific correlation cluster (Figs. 6 and 7, Additional file 7: Table S7).

LncRNA and mRNA co-expression analysis: normal ipRGCs vs. injured ipRGCs

We did not find any correlated lncRNA- mRNA pair in the set of differentially-expressed transcripts in this group comparison.

LncRNA and mRNA co-expression analysis: normal ooDSGCs vs. injured ooDSGCs

Co-expressing pairs comprised 19 lncRNAs whose expression was correlated with a total of 395 mRNAs (Fig. 6a, Additional file 6: Table S6), and these mRNAs were grouped into four clusters. Functional analysis of the mRNAs in each cluster revealed enrichment of several GO "Biological Processes" and "Molecular Functions" terms including "calcium ion binding", "nervous system development", "intrinsic apoptotic signaling pathway in response to endoplasmic reticulum stress", "response to endoplasmic reticulum stress," and "neuron projection development" (Fig. 6a, Additional file 7: Table S7). Figures 6b and 6c show sub-groups of protein-coding genes

352 from cluster 2 (e.g. *Atf4, Ddit3* and *Trib3*) that are associated with regulating RGC death after
353 injury (29, 30).

354 LncRNA and mRNA co-expression analysis: injured ipRGCs vs. injured ooDSGCs

355 Findings showed that 320 mRNAs were correlated with 14 lncRNAs and grouped in two clusters
356 (Fig. 7a, Additional file 6: Table S6). The mRNAs in these clusters were significantly enriched
357 in GO terms such as "protein catabolic process" and "response to unfolded protein and regulation
358 of translation" (Fig. 7a, Additional file 7: Table S7).

359 LncRNA and mRNA co-expression analysis: normal ipRGCs vs. normal ooDSGCs

360 Co-expressing pairs including 16 lncRNAs correlated with a total of 331 mRNAs, and these
361 mRNAs were grouped in two clusters (Figure 7b, Additional file 7: Table S6). The protein-
362 coding genes in these clusters were significantly enriched in GO terms such as "calcium ion
363 binding", "nervous system development", "neuron migration," and "axon guidance" (Fig. 7b,
364 Additional file 7: Table S7).

365

366 **Discussion**

367 RGCs comprising distinct subtypes have been studied widely to probe mechanisms governing
368 cell type specification during development as well as neuronal survival after injury. ipRGCs are
369 a group of neurons that express the photopigment melanopsin (31-33). They have unique
370 molecular and functional features quite distinct from other RGCs. In mice, although ipRGCs are
371 generated as early as embryonic day 1, they follow a delayed developmental time course relative
372 to other RGCs. ipRGC neurogenesis extends beyond that of other RGCs, and ipRGCs begin

innervating their targets at postnatal ages, unlike most RGCs, which innervate their targets embryonically (34). Another unique feature of ipRGCs is that they are resilient to various types of insults, including axonal injury.

DSGCs are a major RGC type that represent approximately 20 % of the total RGC population (35, 36). DSGCs are broadly grouped based on two criteria. First, they either respond to both light onset and offset (ON-OFF) or just to the former (ON). Second, they prefer different directions of motion, giving rise to four types of ON-OFF DSGCs and three types of ON DSGCs. The ooDSGCs detect motion in one of four cardinal axes dorsal, ventral, temporal, and nasal directions (37, 38). Previous studies have also shown that the ventrally-tuned ooDSGCs are fluorescently tagged with reporter in the HB9-GFP BAC transgenic mice. Using this mouse line, it was shown that these ooDSGCs are particularly vulnerable to axotomy (9).

LncRNAs are emerging as major controllers of gene expression networks in developmental, physiological, and pathological processes. Many lncRNAs show tissue- and cell-specific expression, particularly in the nervous system. LncRNAs regulate the transcription of proximal and distal protein-coding genes in *cis* and in *trans*, respectively. LncRNAs can either activate or repress protein-coding genes through different mechanisms (25, 39). For example, lncRNAs can trigger gene transcription by recruiting chromatin activation complex such as TrxG/MLL, leading to deposition of histone 3 lysine 4 trimethylation (H3K4me3) at the gene promoters. Alternatively, lncRNAs can regulate nuclear positioning of enhancer, potentiating the enhancer to induce expression of the target genes. Others have shown that distinct lncRNAs interact with the chromatin remodeler PRC2 complex, resulting in methylation of histone H3 at lysine 27 (H3K27me3) and repression of gene transcription (40-43). However, despite the recognition of lncRNAs as a major regulator of gene expression during development and in pathological

conditions, the extent to which lncRNAs regulate RGC development and survival remains largely unknown.

We identified numerous lncRNAs that were differentially expressed between normal ipRGCs and normal ooDSGCs. As mentioned above, many of these lncRNAs lie in close proximity to protein-coding genes that encode RGC type-specific transcription factors, including *Eomes,* *Brn3a,* and *Brn3c.* However, it remains unknown whether these differentially expressed lncRNAs in fact regulate the expression of these transcription factors and control RGC development.

Another notable finding in this study is the dozens of lncRNAs whose expressions were altered in response to axonal injury. Nearest-neighbor analysis identified apoptosis-related genes that are close neighbors of these lncRNAs. One example is the gene *Ecel1*, which has been studied extensively for its role in regulating RGC death after injury (44). Ecel1 protein, a membrane-bound metalloprotease, has been shown prevent the activation of signaling pathways associated with apoptosis (44, 45). Co-expression of *RP23-416O18.4* and *Ecel1* seen in our nearest-neighbor analysis was similarly observed in two previous studies (13, 46). A single cell RNA-sequencing performed on mouse RGCs has shown that *RP23-416O18.4* and *Ecel1* have the same expression pattern across different time-points after axonal injury (13). In another study, RNA-seq was performed on whole retinas, and the results showed that these two genes are among the top 20 upregulated genes after optic nerve crush (46).

Although many lncRNAs are known to act in *cis* and regulate expression of their nearby genes, it is worth noting that lncRNAs can also act in *trans*, distant from their synthesis sites. One example is lncRNA *RP23-471B6.2* (also knowns *lnc-NR2F1*). We found that expression of this

lncRNA was higher in injured ipRGCs compared to ooDSGCs. Given its genomic location, it was suggested that this lncRNA is a potential *cis* regulator of its gene neighbor *Nr2f1* (Additional file 4: Table S4), which encodes a transcription factor involved in nervous system development and neuron migration. However, a recent study has suggested that rather than regulating *Nr2f1*, this lncRNA acts *in trans* and regulates transcription of multiple neuronal genes, including several autism-associated genes, leading to regulation of neuronal cell maturation (47). Intriguingly, we found that this lncRNA is correlated to 29 genes (either positively or negatively) (Additional file 6: Table S6), indicating a potential role of this lncRNA in promoting gene regulation *in trans*.

In our analysis, lncRNA *Neat1* was detected exclusively in injured ipRGCs. A previous study using spinal cord neural progenitor cells showed that *Neat1* regulates neuronal differentiation, migration and apoptosis (48). The authors also showed that overexpression of *Neat1* induces expression of Wnt/β-catenin signaling molecules including Wisp1, Wnt5a, and Wnt2. Moreover, overexpression of *Neat1* prevented apoptotic death of spinal cord neural progenitor cells in an Wnt/β-catenin dependent manner (48). Since the Wnt/β-catenin pathway is known to promote RGC survival and axon regeneration (49), these observations raise a possibility that *Neat1* regulates the Wnt/β-catenin signaling pathway and contributes to promoting ipRGC axon regeneration and survival.

Another lncRNA worth noting is *Malat1*. Our data show that *Malat1* is expressed at a considerably higher level in injured ipRGCs compared to injured ooDSGCs. Pearson correlation lncRNA-mRNA analysis identified that the gene most correlated with *Malat1* was *Anp32b* ($r = 0.93$), an anti-apoptotic protein which functions as an inhibitor of caspase-3 (50). Moreover, our nearest-neighbor gene analysis identified *Scyl1*, a regulator of neuronal function and survival, as

441 a *Malat1* neighbor (51). Previous studies have shown that *Malat1* has a protective effect and
442 regulates RGC survival under different pathological conditions, including glaucoma (52, 53).
443 These observations raise a possibility that *Malat1* regulates *Anp32b* and/or *Scyl1* and ultimately
444 promotes ipRGC survival.

445 Guilt-by-association analysis suggested that lncRNAs may be functionally correlated to protein
446 coding genes enriched in specific "Biological Processes" and "Molecular Functions". Notably,
447 some lncRNAs were correlated with genes significantly enriched in "Biological Processes"
448 related to apoptotic pathways (Fig. 6). Genes associated with RGC death, including *Atf4, Ddit3,*
449 *Chac1* and *Trib3,* were previously shown to be highly expressed in the injured ooDSGCs (7). In
450 our present study, we found that these genes were positively correlated with the lncRNA
451 *Brip1os*, lncRNA *RP23-407N2.2,* and lncRNA *Dubr* (Fig. 6b and 6c, Additional file 6: Table
452 S6).

453 Insulin growth factor-1 (Igf1) is an anti-apoptotic gene highly expressed in the injured ipRGCs
454 (7). *Igf1* was positively correlated with the lncRNAs *RP23-471B6.2* and *RP23-83I13.10*
455 (Additional file 6: Table S6). LncRNA *RP23-83I13.10* was also positively correlated with *Gpx3*,
456 a gene known to ameliorate oxidative stress (54) and also highly enriched in the injured ipRGCs
457 (7). We also observed regeneration-associated genes, including *Nrn1* and *Spp1,* which were
458 correlated with lncRNAs in our analysis (55, 56). *Nrn1*, a gene downregulated in the injured
459 ooDSGCs, was positively correlated with the novel lincRNA *XLOC_036842* (Additional file 6:
460 Table S6), raising the possibility that these lncRNAs may regulate expression of multiple genes
461 in RGCs after injury. We note however, that our assumptions on the functional roles of lncRNAs
462 remain speculative, and whether they in fact act to regulate gene expression, RGC specification,
463 and survival remains to be determined.

Conclusions

In summary, our study has provided the first identification of lncRNAs expressed in two RGC subtypes that are molecularly, physiologically, and functionally distinct from each other. The data from this study could form the foundation for further exploration of lncRNAs and their potential as regulators of retinal cell development and survival after injury.

List of abbreviations

LncRNAs: long noncoding RNAs

RGCs: retinal ganglion cells

OoDSGCs: ON-OFF direction-selective RGCs

IpRGCs: intrinsically photosensitive RGCs

LincRNAs: long intergenic noncoding RNAs

AS lncRNAs: antisense long noncoding RNAs

CNS: central nervous system

DSGCs: direction selective-RGCs

RNA-seq: RNA-sequencing

FPKM: Fragments Per Kilobase Million

DE: differential expression/ differentially expressed

GO: Gene ontology

RT-PCR: Reverse transcription PCR

ON-OFF: light onset and offset

Figure captions

Fig. 1 LncRNA transcriptome of ipRGCs and ooDSGCs. (**a**) Schematic of procedure used for lncRNA identification. Venn diagram showing the number of lncRNAs (**b**) and protein-coding mRNAs (**c**) expressed in ipRGCs and ooDSGCs under normal and injury (i.e. optic nerve crush) conditions.

Fig. 2 LncRNA expression level in ipRGCs and ooDSGCs. Abundance of lncRNAs compared to the protein-coding mRNAs detected in ipRGCs (**a** and **b**) and ooDSGCs (**c** and **d**) under normal and injury conditions. AS, antisense; lincRNA, long intergenic noncoding.

Fig. 3 Genomic features of lncRNAs detected in ipRGCs and ooDSGCs. Comparative analysis of the length distribution (**a**) and number of exons (**b**) of the lncRNAs and protein-coding mRNAs detected in ipRGCs and ooDSGCs.AS, antisense; lincRNA, long intergenic noncoding.

Fig. 4 Heat maps showing lncRNAs differentially expressed in the two RGC types in injury and normal conditions. (**a**) Injured ipRGCs vs. normal ipRGCs; (**b**) Injured ooDSGCs vs. normal ooDSGCs; (**c**) Injured ooDSGCs vs. injured ipRGCs; (D) Normal ooDSGCs vs. normal ipRGCs. Expression values were based on Z-score normalized FPKM for each lncRNA. Rep, replicate.

Fig. 5 Gene ontology enrichment analysis of lncRNAs' nearby genes. Top GO "Biological Process" and "Molecular Function" terms (p-value < 0.05) assigned to the mRNAs located within 300 kb upstream or downstream of the differentially expressed (DE) lncRNAs (**a-d**). DE lncRNAs between injured ipRGCs vs. normal ipRGCs (**a**); injured ooDSGCs vs. normal ooDSGCs (**b**); injured ooDSGCs vs. injured ipRGCs (**c**); normal ooDSGCs vs. normal ipRGCs (**d**). The color scale indicates that the expression of lncRNA is upregulated (red; positive log fold

change), downregulated (green; negative log fold change), or not significantly changed (yellow, log fold change is zero) in each RGC comparison.

Fig. 6 Biological associations arising from the lncRNAs correlated with genes in the injured *vs.* normal ooDSGCs comparison. The differentially-expressed (DE) mRNAs co-expressed with the DE lncRNAs across the four RGC groups were selected ($r > 0.9$ or $r < -0.9$) and used for gene enrichment analysis based on Gene Ontology "Biological Process" (BP) and "Molecular Function" (MF) terms (p-value < 0.05). (**a**) Heat map with correlated lncRNAs (columns) and mRNA (rows) are shown. Five terms among the top ten GO enriched terms in each cluster are shown on the right. (**b-c**) Heat map displaying the correlation between the lncRNAs and a subset of mRNAs from the cluster 2 that were enriched in the BP terms "intrinsic apoptotic signaling pathway in response to endoplasmic reticulum stress" (**b**) and "response to endoplasmic reticulum stress" (**c**). Red to blue Pearson Correlation scale indicates the degree to which mRNA expression is positively (dark red), negatively (dark blue), or not correlated with the expression of the respective lncRNA.

Fig. 7 Biological associations arising from the lncRNAs correlated with genes in the injured and normal RGCs comparisons. The DE mRNAs co-expressed with the DE lncRNAs across the four RGC groups were selected ($r > 0.9$ or $r < -0.9$) and used for gene enrichment analysis based on Gene Ontology "Biological Process" and "Molecular Function" terms (p-value < 0.05). Heat map with correlated lncRNAs (columns) and mRNA (rows) are shown for injured ooDSGCs vs. injured ipRGCs (**a**) and normal ooDSGCs vs. normal ipRGCs (**b**) comparison. Five terms among the top ten enriched terms in each cluster are shown at right. Red to blue Pearson Correlation scale indicates the degree to which mRNA expression is positively (dark red), negatively (dark blue) or not correlated with the expression of the respective lncRNA.

Declarations

Ethics approval and consent to participate

Mouse procedures were performed in compliance with protocols approved by the Institutional Animal Care and Use Committee (IACUC) at University of Miami Miller School of Medicine (Permit Number: 19-150). Work carried out in this current study was in compliance with relevant guidelines and regulations including those of University of Miami Miller School of Medicine.

Consent for publication

Not applicable.

Availability of data and materials

All data analyzed during this study are included in this article and its supplementary information files. The RNA-seq data from the injured and normal ipRGCs and ooDSGCs used in this article is deposited under the accession number GEO: GSE115661(7). The RNA-seq data from the whole retina was downloaded from Sequence Read Archive (SRA) PRJNA514424 (22).

Competing interests

No potential conflict of interest was reported by the authors.

Funding

This work was supported by grants from the National Eye Institute 1R01EY022961 (K.K.P.), NEI 1U01EY027257 (K.K.P), DOD W81XWH-19-1-0736 (K.K.P), DOD W81XWH-19-1-0845 (K.K.P and A.A), The Miami Project to Cure Paralysis, and the Buoniconti Fund (K.K.P) and Glaucoma Research Foundation (K.K.P).

Authors' contributions

A.C.A. and K.K.P. conceived the research. A.C.A. and K. L. performed molecular experiments. A.C.A and F.B. performed data analysis. A.C.A and K.K.P. wrote the paper. R.S. aided in discussing the results.

Acknowledgements

The authors thank the Flow Cytometry Shared Resource, at University of Miami, Sylvester Comprehensive Cancer Center for the support with cell sorting.

References

1. Cabili MN, Trapnell C, Goff L, Koziol M, Tazon-Vega B, Regev A, et al. Integrative annotation of human large intergenic noncoding RNAs reveals global properties and specific subclasses. Genes Dev. 2011;25(18):1915-27.
2. Yan L, Yang M, Guo H, Yang L, Wu J, Li R, et al. Single-cell RNA-Seq profiling of human preimplantation embryos and embryonic stem cells. Nat Struct Mol Biol. 2013;20(9):1131-9.
3. Sweeney NT, James KN, Nistorica A, Lorig-Roach RM, Feldheim DA. Expression of transcription factors divides retinal ganglion cells into distinct classes. J Comp Neurol. 2019;527(1):225-35.
4. Mao CA, Li H, Zhang Z, Kiyama T, Panda S, Hattar S, et al. T-box transcription regulator Tbr2 is essential for the formation and maintenance of Opn4/melanopsin-expressing intrinsically photosensitive retinal ganglion cells. J Neurosci. 2014;34(39):13083-95.
5. Sajgo S, Ghinia MG, Brooks M, Kretschmer F, Chuang K, Hiriyanna S, et al. Molecular codes for cell type specification in Brn3 retinal ganglion cells. Proc Natl Acad Sci U S A. 2017;114(20):E3974-E83.
6. Nguyen-Ba-Charvet KT, Rebsam A. Neurogenesis and Specification of Retinal Ganglion Cells. Int J Mol Sci. 2020;21(2).
7. Bray ER, Yungher BJ, Levay K, Ribeiro M, Dvoryanchikov G, Ayupe AC, et al. Thrombospondin-1 Mediates Axon Regeneration in Retinal Ganglion Cells. Neuron. 2019;103(4):642-57 e7.
8. Cui Q, Ren C, Sollars PJ, Pickard GE, So KF. The injury resistant ability of melanopsin-expressing intrinsically photosensitive retinal ganglion cells. Neuroscience. 2015;284:845-53.
9. Duan X, Qiao M, Bei F, Kim IJ, He Z, Sanes JR. Subtype-specific regeneration of retinal ganglion cells following axotomy: effects of osteopontin and mTOR signaling. Neuron. 2015;85(6):1244-56.
10. VanderWall KB, Lu B, Alfaro JS, Allsop AR, Carr AS, Wang S, et al. Differential susceptibility of retinal ganglion cell subtypes in acute and chronic models of injury and disease. Sci Rep. 2020;10(1):17359.
11. Perez de Sevilla Muller L, Sargoy A, Rodriguez AR, Brecha NC. Melanopsin ganglion cells are the most resistant retinal ganglion cell type to axonal injury in the rat retina. Plos One. 2014;9(3):e93274.
12. Berry M, Ahmed Z, Logan A. Return of function after CNS axon regeneration: Lessons from injury-responsive intrinsically photosensitive and alpha retinal ganglion cells. Prog Retin Eye Res. 2019;71:57-67.
13. Tran NM, Shekhar K, Whitney IE, Jacobi A, Benhar I, Hong G, et al. Single-Cell Profiles of Retinal Ganglion Cells Differing in Resilience to Injury Reveal Neuroprotective Genes. Neuron. 2019;104(6):1039-55 e12.
14. Rheaume BA, Jereen A, Bolisetty M, Sajid MS, Yang Y, Renna K, et al. Single cell transcriptome profiling of retinal ganglion cells identifies cellular subtypes. Nat Commun. 2018;9(1):2759.
15. Dobin A, Davis CA, Schlesinger F, Drenkow J, Zaleski C, Jha S, et al. STAR: ultrafast universal RNA-seq aligner. Bioinformatics. 2013;29(1):15-21.

16. daSilva LF, Beckedorff FC, Ayupe AC, Amaral MS, Mesel V, Videira A, et al. Chromatin Landscape Distinguishes the Genomic Loci of Hundreds of Androgen-Receptor-Associated LincRNAs From the Loci of Non-associated LincRNAs. Front Genet. 2018;9:132.
17. Trapnell C, Hendrickson DG, Sauvageau M, Goff L, Rinn JL, Pachter L. Differential analysis of gene regulation at transcript resolution with RNA-seq. Nat Biotechnol. 2013;31(1):46-53.
18. Kang YJ, Yang DC, Kong L, Hou M, Meng YQ, Wei L, et al. CPC2: a fast and accurate coding potential calculator based on sequence intrinsic features. Nucleic Acids Res. 2017;45(W1):W12-W6.
19. Li B, Dewey CN. RSEM: accurate transcript quantification from RNA-Seq data with or without a reference genome. BMC Bioinformatics. 2011;12:323.
20. Huang da W, Sherman BT, Lempicki RA. Systematic and integrative analysis of large gene lists using DAVID bioinformatics resources. Nat Protoc. 2009;4(1):44-57.
21. Sauvageau M, Goff LA, Lodato S, Bonev B, Groff AF, Gerhardinger C, et al. Multiple knockout mouse models reveal lincRNAs are required for life and brain development. Elife. 2013;2:e01749.
22. Wan Y, Liu XY, Zheng DW, Wang YY, Chen H, Zhao XF, et al. Systematic identification of intergenic long-noncoding RNAs in mouse retinas using full-length isoform sequencing. Bmc Genomics. 2019;20.
23. Baden T, Berens P, Franke K, Roman Roson M, Bethge M, Euler T. The functional diversity of retinal ganglion cells in the mouse. Nature. 2016;529(7586):345-50.
24. Derrien T, Johnson R, Bussotti G, Tanzer A, Djebali S, Tilgner H, et al. The GENCODE v7 catalog of human long noncoding RNAs: analysis of their gene structure, evolution, and expression. Genome Res. 2012;22(9):1775-89.
25. Gil N, Ulitsky I. Regulation of gene expression by cis-acting long non-coding RNAs. Nat Rev Genet. 2020;21(2):102-17.
26. Arons MH, Lee K, Thynne CJ, Kim SA, Schob C, Kindler S, et al. Shank3 Is Part of a Zinc-Sensitive Signaling System That Regulates Excitatory Synaptic Strength. J Neurosci. 2016;36(35):9124-34.
27. Gan L, Wang SW, Huang Z, Klein WH. POU domain factor Brn-3b is essential for retinal ganglion cell differentiation and survival but not for initial cell fate specification. Dev Biol. 1999;210(2):469-80.
28. Jain V, Ravindran E, Dhingra NK. Differential expression of Brn3 transcription factors in intrinsically photosensitive retinal ganglion cells in mouse. J Comp Neurol. 2012;520(4):742-55.
29. Hu Y, Park KK, Yang L, Wei X, Yang Q, Cho KS, et al. Differential Effects of Unfolded Protein Response Pathways on Axon Injury-Induced Death of Retinal Ganglion Cells. Neuron. 2012;73(3):445-52.
30. Yasuda M, Tanaka Y, Ryu M, Tsuda S, Nakazawa T. RNA Sequence Reveals Mouse Retinal Transcriptome Changes Early after Axonal Injury. Plos One. 2014;9(3).
31. Aranda ML, Schmidt TM. Diversity of intrinsically photosensitive retinal ganglion cells: circuits and functions. Cell Mol Life Sci. 2020.
32. Do MTH. Melanopsin and the Intrinsically Photosensitive Retinal Ganglion Cells: Biophysics to Behavior. Neuron. 2019;104(2):205-26.
33. Pickard GE, Sollars PJ. Intrinsically photosensitive retinal ganglion cells. Rev Physiol Biochem Pharmacol. 2012;162:59-90.

673 34. McNeill DS, Sheely CJ, Ecker JL, Badea TC, Morhardt D, Guido W, et al. Development
674 of melanopsin-based irradiance detecting circuitry. Neural Dev. 2011;6:8.
675 35. Sanes JR, Masland RH. The types of retinal ganglion cells: current status and
676 implications for neuronal classification. Annu Rev Neurosci. 2015;38:221-46.
677 36. Liu J. The Anatomy and Physiology of Direction-Selective Retinal Ganglion Cells. In:
678 Kolb H, Fernandez E, Nelson R, editors. Webvision: The Organization of the Retina and Visual
679 System. Salt Lake City (UT)1995.
680 37. Oyster CW, Barlow HB. Direction-selective units in rabbit retina: distribution of
681 preferred directions. Science. 1967;155(3764):841-2.
682 38. Dhande OS, Stafford BK, Franke K, El-Danaf R, Percival KA, Phan AH, et al. Molecular
683 Fingerprinting of On-Off Direction-Selective Retinal Ganglion Cells Across Species and
684 Relevance to Primate Visual Circuits. J Neurosci. 2019;39(1):78-95.
685 39. Kopp F, Mendell JT. Functional Classification and Experimental Dissection of Long
686 Noncoding RNAs. Cell. 2018;172(3):393-407.
687 40. Rinn JL, Kertesz M, Wang JK, Squazzo SL, Xu X, Brugmann SA, et al. Functional
688 demarcation of active and silent chromatin domains in human HOX loci by noncoding RNAs.
689 Cell. 2007;129(7):1311-23.
690 41. Khalil AM, Guttman M, Huarte M, Garber M, Raj A, Rivea Morales D, et al. Many
691 human large intergenic noncoding RNAs associate with chromatin-modifying complexes and
692 affect gene expression. Proc Natl Acad Sci U S A. 2009;106(28):11667-72.
693 42. Beckedorff FC, Ayupe AC, Crocci-Souza R, Amaral MS, Nakaya HI, Soltys DT, et al.
694 The intronic long noncoding RNA ANRASSF1 recruits PRC2 to the RASSF1A promoter,
695 reducing the expression of RASSF1A and increasing cell proliferation. PLoS Genet.
696 2013;9(8):e1003705.
697 43. Videira A, Beckedorff FC, daSilva LF, Verjovski-Almeida S. PVT1 signals an androgen-
698 dependent transcriptional repression program in prostate cancer cells and a set of the repressed
699 genes predicts high-risk tumors. Cell Commun Signal. 2021;19(1):5.
700 44. Sato K, Shiga Y, Nakagawa Y, Fujita K, Nishiguchi KM, Tawarayama H, et al. Ecel1
701 Knockdown With an AAV2-Mediated CRISPR/Cas9 System Promotes Optic Nerve Damage-
702 Induced RGC Death in the Mouse Retina. Invest Ophthalmol Vis Sci. 2018;59(10):3943-51.
703 45. Kaneko A, Kiryu-Seo S, Matsumoto S, Kiyama H. Damage-induced neuronal
704 endopeptidase (DINE) enhances axonal regeneration potential of retinal ganglion cells after optic
705 nerve injury. Cell Death Dis. 2017;8(6):e2847.
706 46. Chen J, Zhang L, Liu L, Yang X, Wu F, Gan X, et al. Acupuncture Treatment Reverses
707 Retinal Gene Expression Induced by Optic Nerve Injury via RNA Sequencing Analysis. Front
708 Integr Neurosci. 2019;13:59.
709 47. Ang CE, Ma Q, Wapinski OL, Fan S, Flynn RA, Lee QY, et al. The novel lncRNA lnc-
710 NR2F1 is pro-neurogenic and mutated in human neurodevelopmental disorders. Elife. 2019;8.
711 48. Cui Y, Yin Y, Xiao Z, Zhao Y, Chen B, Yang B, et al. LncRNA Neat1 mediates miR-
712 124-induced activation of Wnt/beta-catenin signaling in spinal cord neural progenitor cells. Stem
713 Cell Res Ther. 2019;10(1):400.
714 49. Patel AK, Park KK, Hackam AS. Wnt signaling promotes axonal regeneration following
715 optic nerve injury in the mouse. Neuroscience. 2017;343:372-83.
716 50. Shen SM, Yu Y, Wu YL, Cheng JK, Wang LS, Chen GQ. Downregulation of ANP32B, a
717 novel substrate of caspase-3, enhances caspase-3 activation and apoptosis induction in myeloid
718 leukemic cells. Carcinogenesis. 2010;31(3):419-26.

51. Kuliyev E, Gingras S, Guy CS, Howell S, Vogel P, Pelletier S. Overlapping Role of SCYL1 and SCYL3 in Maintaining Motor Neuron Viability. J Neurosci. 2018;38(10):2615-30.
52. Yao J, Wang XQ, Li YJ, Shan K, Yang H, Wang YN, et al. Long non-coding RNA MALAT1 regulates retinal neurodegeneration through CREB signaling. EMBO Mol Med. 2016;8(4):346-62.
53. Li HB, You QS, Xu LX, Sun LX, Abdul Majid AS, Xia XB, et al. Long Non-Coding RNA-MALAT1 Mediates Retinal Ganglion Cell Apoptosis Through the PI3K/Akt Signaling Pathway in Rats with Glaucoma. Cell Physiol Biochem. 2017;43(5):2117-32.
54. Lei XG, Zhu JH, Cheng WH, Bao Y, Ho YS, Reddi AR, et al. Paradoxical Roles of Antioxidant Enzymes: Basic Mechanisms and Health Implications. Physiol Rev. 2016;96(1):307-64.
55. Liu X, Sun Y, Li H, Li Y, Li M, Yuan Y, et al. Effect of Spp1 on nerve degeneration and regeneration after rat sciatic nerve injury. BMC Neurosci. 2017;18(1):30.
56. Sharma TP, Liu Y, Wordinger RJ, Pang IH, Clark AF. Neuritin 1 promotes retinal ganglion cell survival and axonal regeneration following optic nerve crush. Cell Death Dis. 2015;6:e1661.

Additional file 1 (.docx):

Table S1. List of primers used in this study.

Additional file 2 (.xlsx):

Table S2. List of lncRNAs detected in ipRGCs and ooDSGCs.

Additional file 3 (.xlsx):

Table S3. List of the lncRNAs detected in normal ipRGCs or in normal ooDSGCs that are also detected in the whole retina.

Additional file 4 (.xlsx):

Table S4. List of the differentially expressed lncRNAs detected from various RGC group comparisons.

Additional file 5 (.xlsx):

Table S5. Top GO "Biological Process" and "Molecular Function" enriched terms (p-value < 0.05) assigned to the mRNAs located within 300 kb upstream or downstream of the differentially expressed lncRNAs.

Additional file 6 (.xlsx):

Table S6. List of lncRNAs with expression correlated to protein coding genes ($r \geq |0.9|$).

Additional file 7 (.xlsx):

Table S7. Top GO "Biological Process" and "Molecular Function" enriched terms (p-value < 0.05) assigned to the protein-coding genes correlated with lncRNA ($r \geq |0.9|$) in each cluster.

Additional file 8: Figures S1-S6 (pfd):

Fig. S1 Subclasses of lncRNAs detected in ipRGCs and ooDSGCs. Venn diagram showing antisense lncRNAs (AS lncRNAs) (**a**), long intergenic noncoding RNAs (lincRNAs) (**b**) and novel lincRNAs (**c**) expressed under normal and injury (i.e. optic nerve crush) conditions.

Fig. S2 Expression level comparison between the whole retina lincRNAs and lncRNAs detected in normal ipRGCs (**a**) and normal ooDSGCs (**b**). Length distribution (**c**) and number of exon (**d**) comparison between the whole retina lincRNAs and lncRNAs detected in ipRGCs and ooDSGCs.

Fig. S3 Validating expression of a novel lincRNA in RGCs. (**a**) Representative images of retinal sections from Thy1-CFP mice showing GFP and RBPMS immunoreactivity. Nearly all GFP+ cells are RBPMS+, indicating that RGCs are specifically labelled in this mouse line. (**b**) Representative FACS plots of dissociated retinal cells expressing CFP. CFP+ and CFP- cells were collected for RNA extraction and RT-qPCR. (**c**) Level of expression of *Thy1* and *Slc17a6*

786 (markers for RGCs) and *Rho* (marker for rods). CFP+ cells show enrichment of RGC genes
787 compared to CFP- cells. Date from three biological replicates (mean ± SD; * p-value < 0.05;
788 unpaired two-tailed t test). (**d**) RT-PCR result for one randomly selected differentially expressed
789 lincRNA (XLOC_034401, isoform TCONS_00067968). XLOC_034401 was significantly
790 upregulated in injured ooDSGCs compared to normal ooDSGCs. RNA from optic nerve crushed
791 Thy1-CFP mice was used for reverse transcription. Primer pair was designed to amplify a
792 fragment spanning one intron. PCR amplicon was confirmed by Sanger sequencing.

793 **Fig. S4** Heat map showing the expression level of protein-coding mRNAs that are neighbors of
794 the differentially expressed lncRNAs. (**a**) Injured ipRGCs vs. normal ipRGCs. (**b**) Injured
795 ooDSGCs vs. normal ooDSGCs. Expression values were based on Z-score normalized FPKM for
796 each mRNA.

797 **Fig. S5** Heat map showing the expression level of protein-coding mRNAs that are neighbors of
798 the differentially expressed lncRNAs. (**a**) Injured ooDSGCs vs. injured ipRGCs. (**b**) Normal
799 ooDSGCs vs. normal ipRGCs. Expression values were based on Z-score normalized FPKM for
800 each mRNA.

801 **Fig. S6** Volcano plot showing the level of gene expression for the protein-coding mRNAs that
802 are neighbors of the differentially expressed lncRNAs. (**a**) Injured ipRGCs vs. normal ipRGCs.
803 (**b**) Injured ooDSGCs vs. normal ooDSGCs. (c) Injured ooDSGCs vs. injured ipRGCs. (**d**)
804 Normal ooDSGCs vs. normal ipRGCs. Red and blue dots indicate top differentially expressed
805 genes; gray dots indicate genes that are not differentially expressed.

806

807

Figures

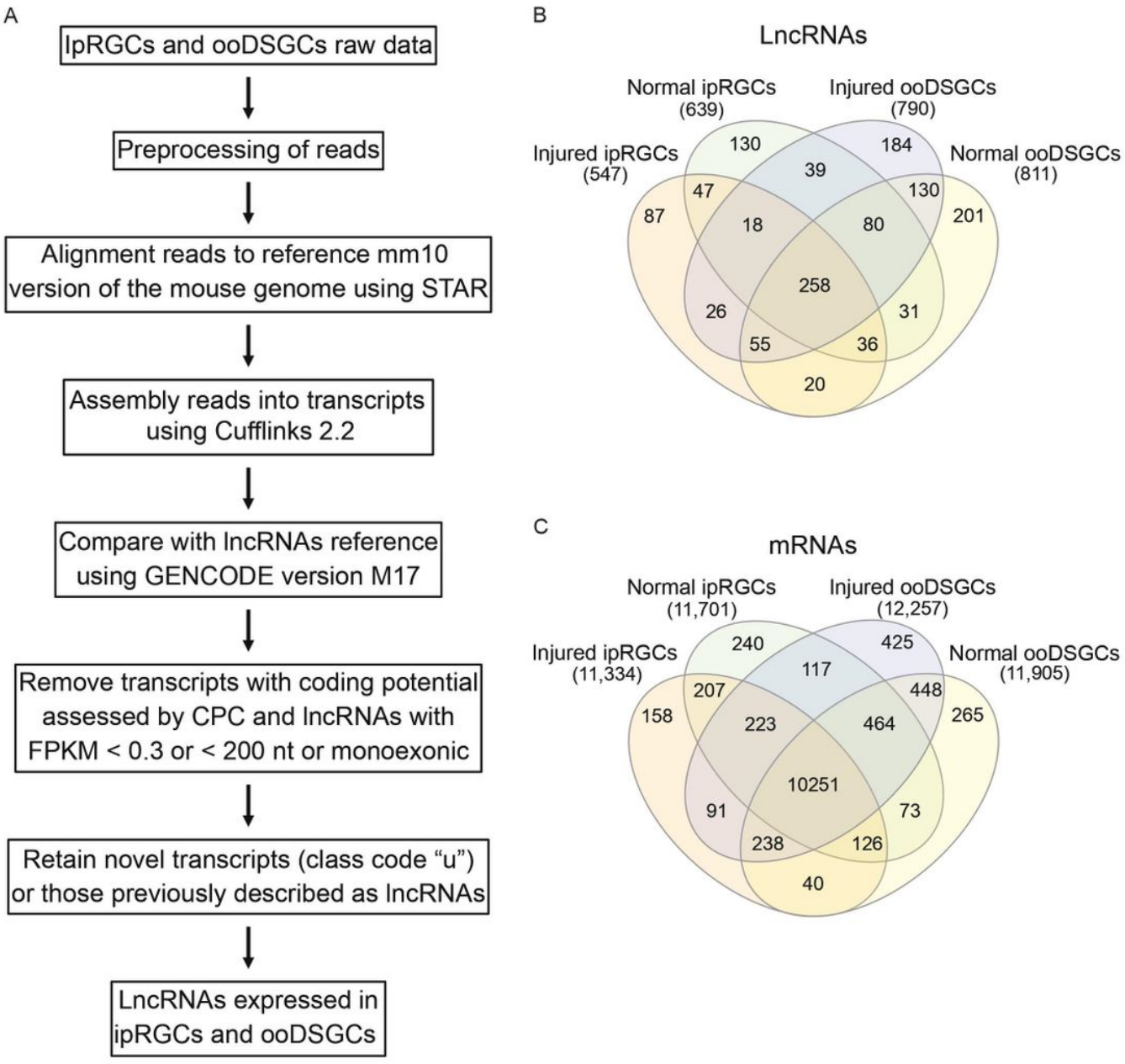

Figure 1

LncRNA transcriptome of ipRGCs and ooDSGCs. (a) Schematic of procedure used for lncRNA identification. Venn diagram showing the number of lncRNAs (b) and protein-coding mRNAs (c) expressed in ipRGCs and ooDSGCs under normal and injury (i.e. optic nerve crush) conditions.

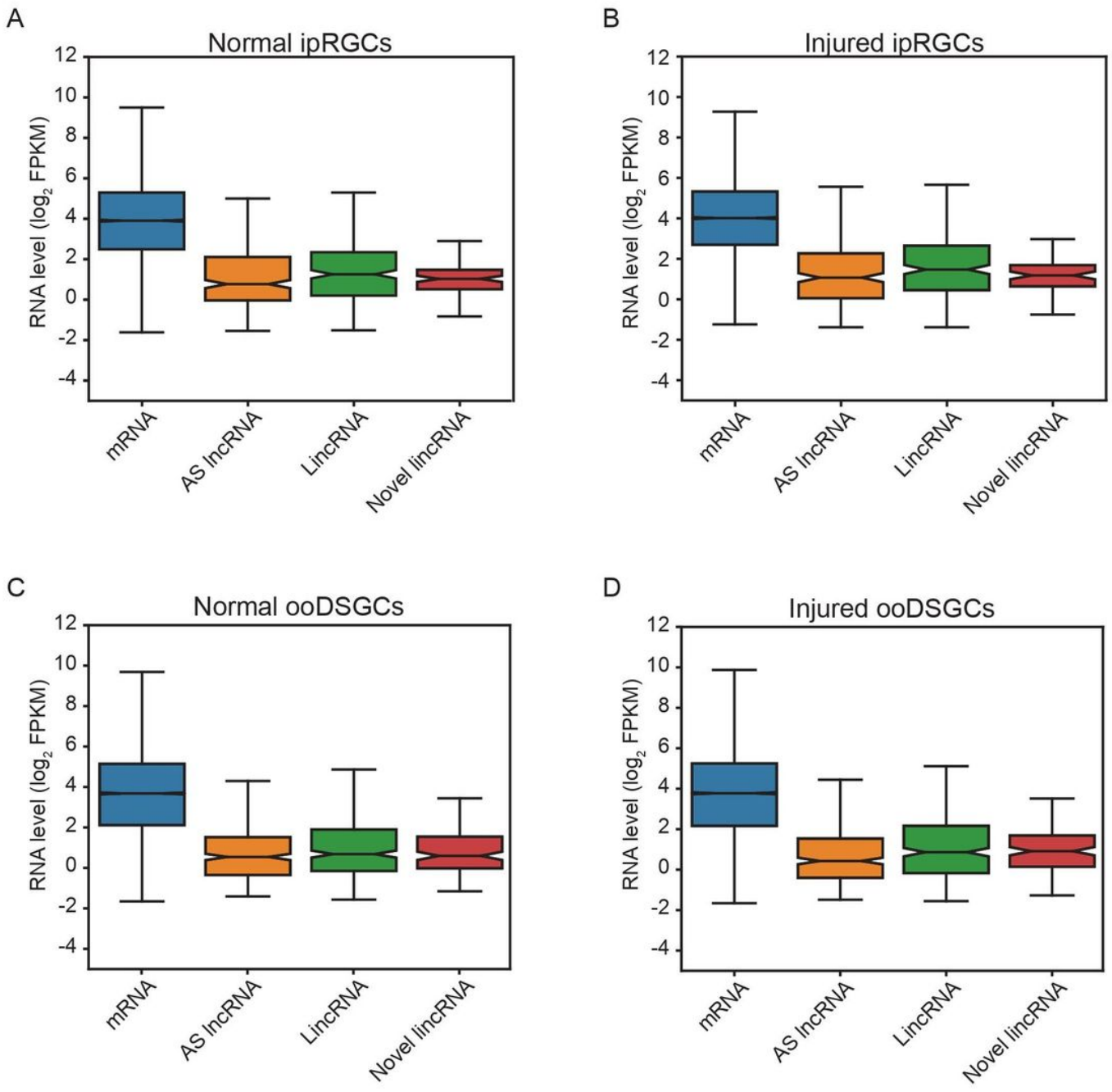

Figure 2

LncRNA expression level in ipRGCs and ooDSGCs. Abundance of lncRNAs compared to the protein-coding mRNAs detected in ipRGCs (a and b) and ooDSGCs (c and d) under normal and injury conditions. AS, antisense; lincRNA, long intergenic noncoding.

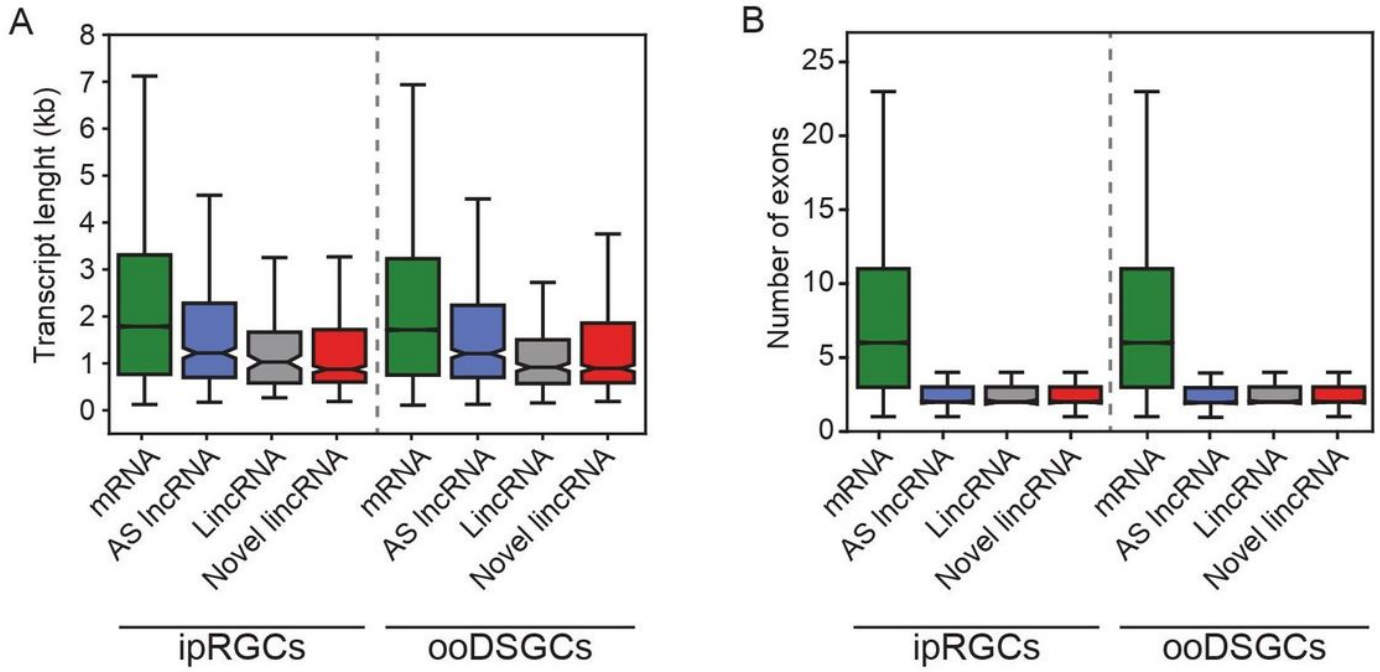

Figure 3

Genomic features of lncRNAs detected in ipRGCs and ooDSGCs. Comparative analysis of the length distribution (a) and number of exons (b) of the lncRNAs and protein-coding mRNAs detected in ipRGCs and ooDSGCs.AS, antisense; lincRNA, long intergenic noncoding.

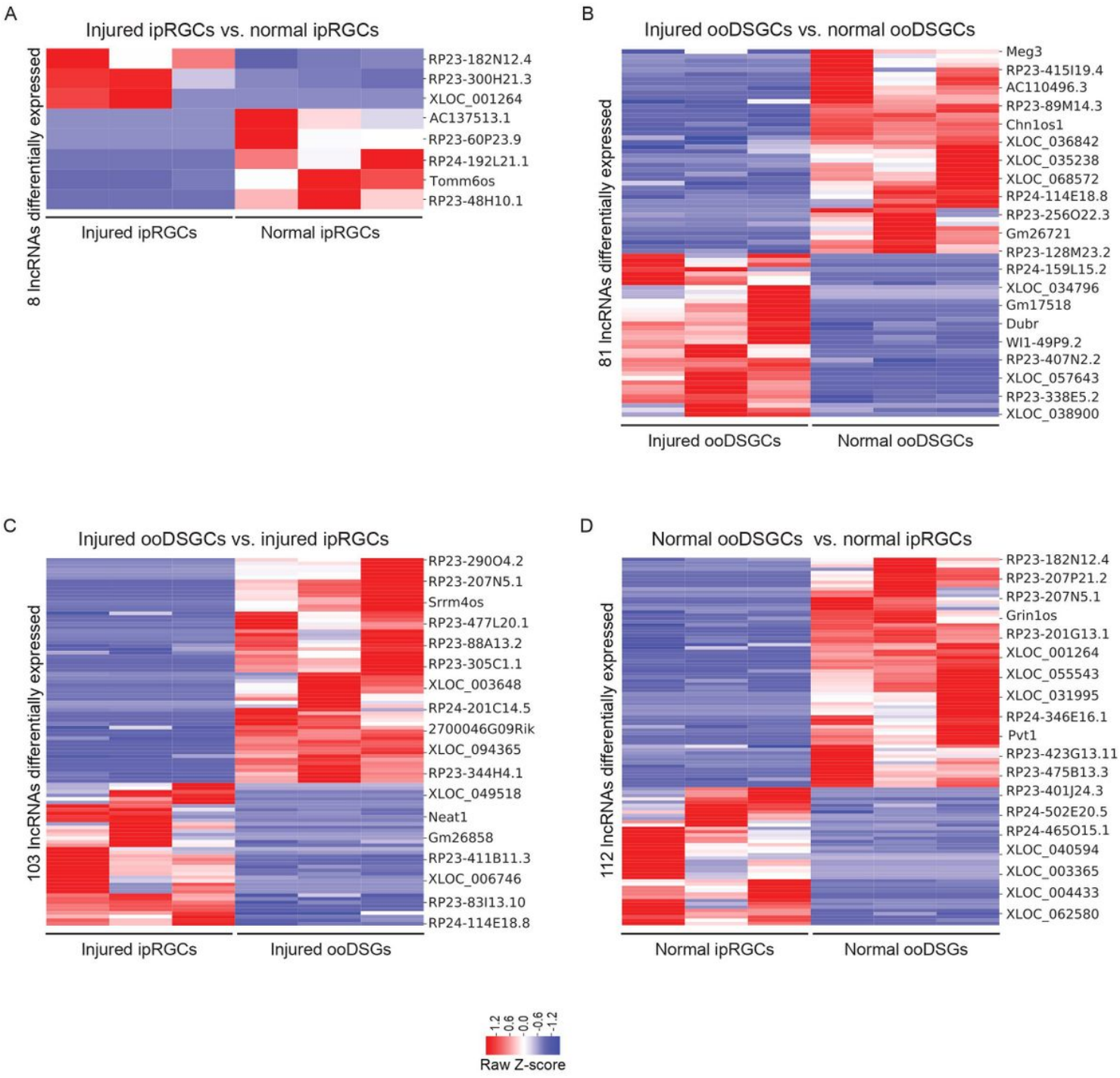

Figure 4

Heat maps showing lncRNAs differentially expressed in the two RGC types in injury and normal conditions. (a) Injured ipRGCs vs. normal ipRGCs; (b) Injured ooDSGCs vs. normal ooDSGCs; (c) Injured ooDSGCs vs. injured ipRGCs; (D) Normal ooDSGCs vs. normal ipRGCs. Expression values were based on Z-score normalized FPKM for each lncRNA. Rep, replicate.

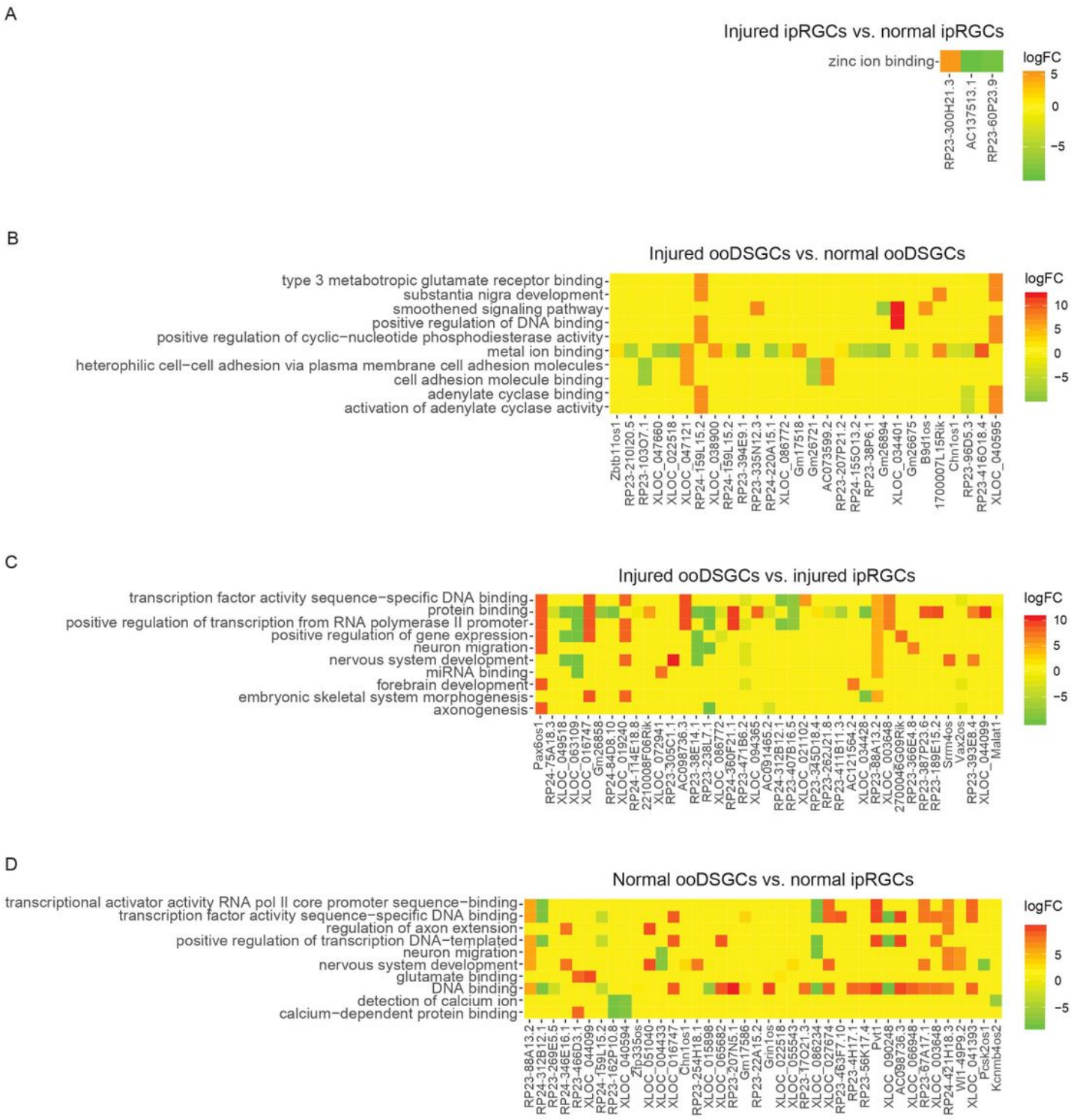

Figure 5

Gene ontology enrichment analysis of lncRNAs' nearby genes. Top GO "Biological Process" and "Molecular Function" terms (p-value < 0.05) assigned to the mRNAs located within 300 kb upstream or downstream of the differentially expressed (DE) lncRNAs (a-d). DE lncRNAs between injured ipRGCs vs. normal ipRGCs (a); injured ooDSGCs vs. normal ooDSGCs (b); injured ooDSGCs vs. injured ipRGCs (c); normal ooDSGCs vs. normal ipRGCs (d). The color scale indicates that the expression of lncRNA is

upregulated (red; positive log fold change), downregulated (green; negative log fold change), or not significantly changed (yellow, log fold change is zero) in each RGC comparison.

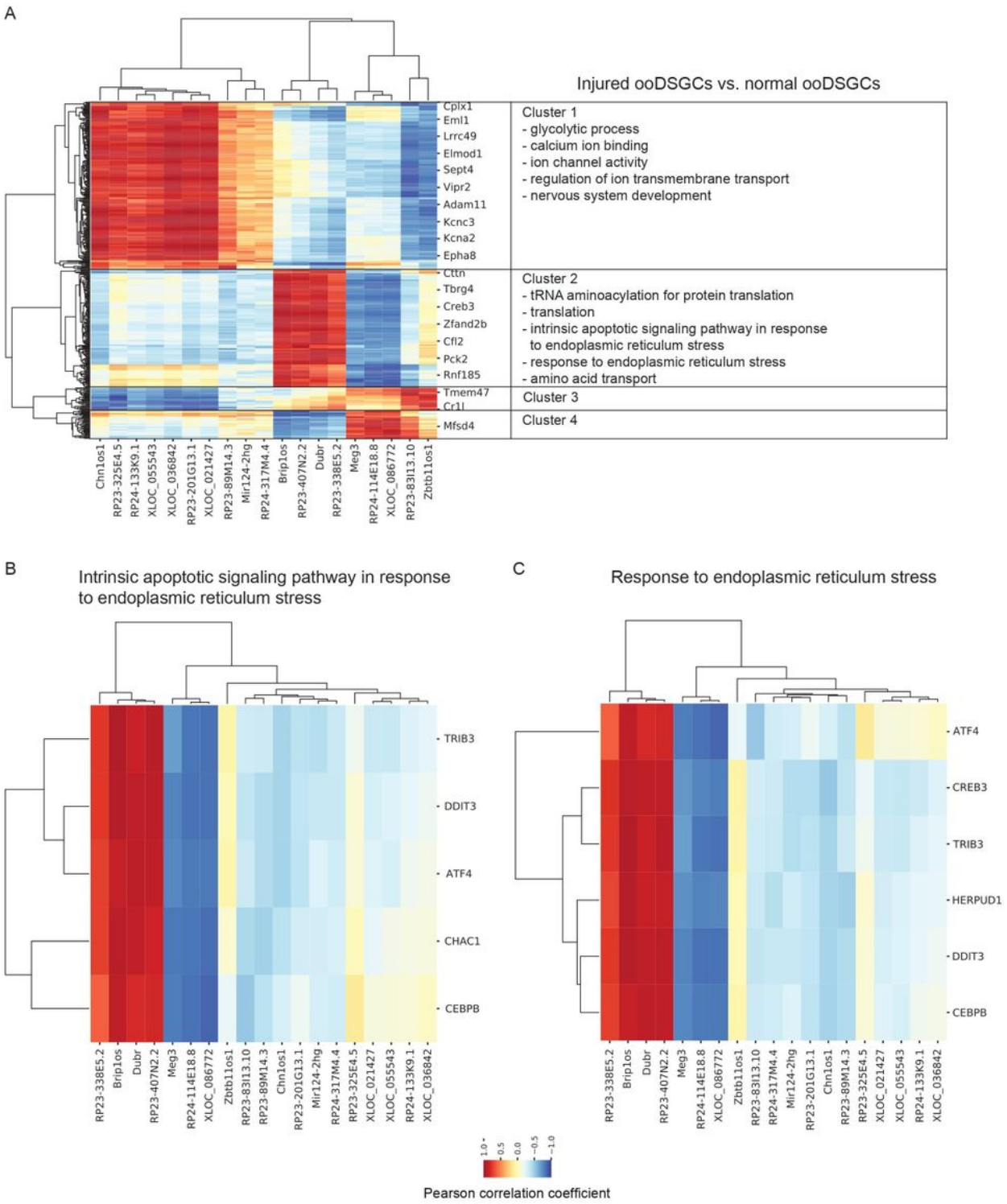

Figure 6

Biological associations arising from the lncRNAs correlated with genes in the injured vs. normal ooDSGCs comparison. The differentially-expressed (DE) mRNAs co-expressed with the DE lncRNAs across the four RGC groups were selected ($r > 0.9$ or $r < -0.9$) and used for gene enrichment analysis

based on Gene Ontology “Biological Process” (BP) and “Molecular Function” (MF) terms (p-value < 0.05). (a) Heat map with correlated lncRNAs (columns) and mRNA (rows) are shown. Five terms among the top ten GO enriched terms in each cluster are shown on the right. (b-c) Heat map displaying the correlation between the lncRNAs and a subset of mRNAs from the cluster 2 that were enriched in the BP terms “intrinsic apoptotic signaling pathway in response to endoplasmic reticulum stress” (b) and “response to endoplasmic reticulum stress” (c). Red to blue Pearson Correlation scale indicates the degree to which mRNA expression is positively (dark red), negatively (dark blue), or not correlated with the expression of the respective lncRNA.

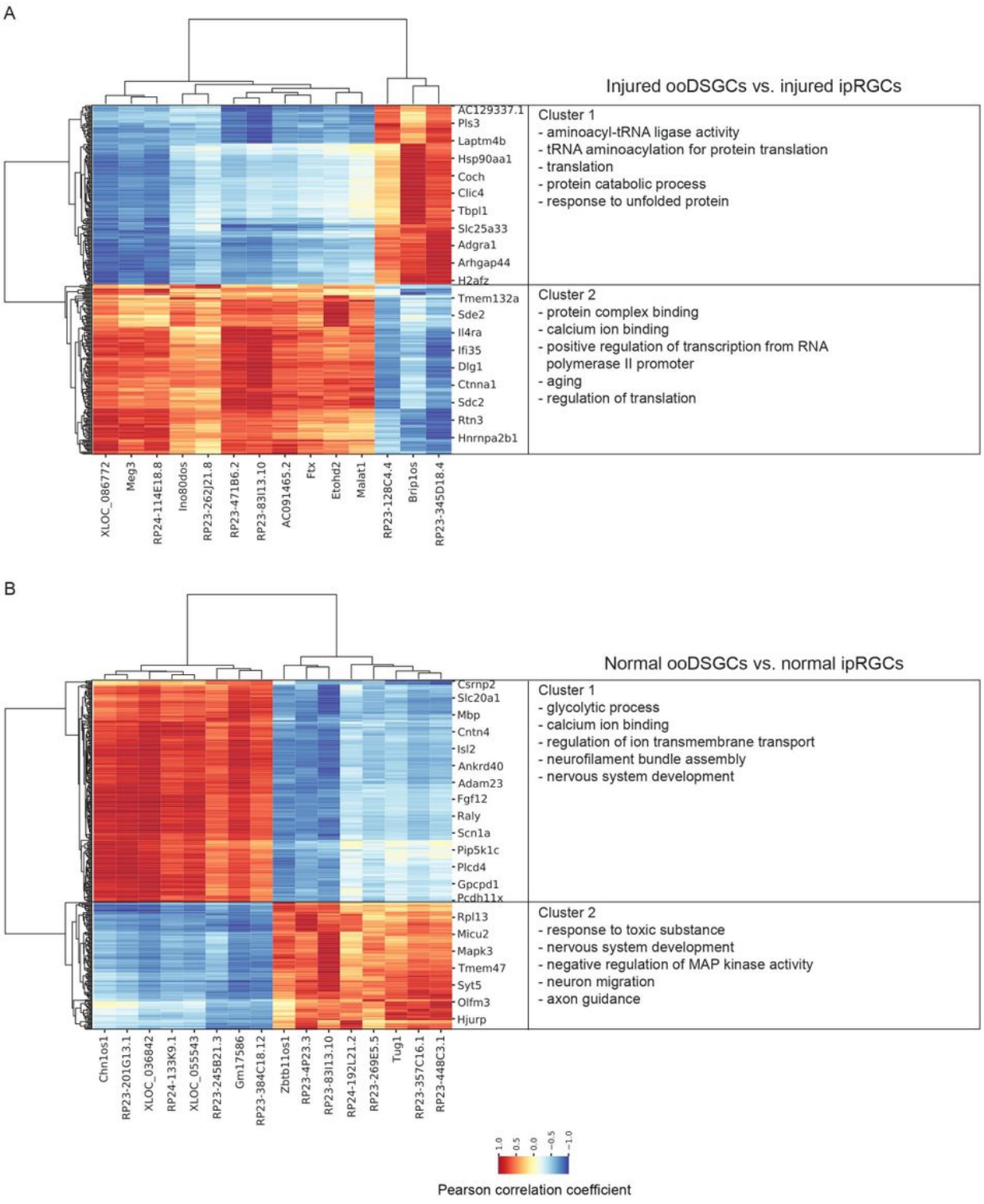

Figure 7

Biological associations arising from the lncRNAs correlated with genes in the injured and normal RGCs comparisons. The DE mRNAs co-expressed with the DE lncRNAs across the four RGC groups were selected ($r > 0.9$ or $r < -0.9$) and used for gene enrichment analysis based on Gene Ontology “Biological Process” and “Molecular Function” terms ($p\text{-value} < 0.05$). Heat map with correlated lncRNAs (columns) and mRNA (rows) are shown for injured ooDSGCs vs. injured ipRGCs (a) and normal ooDSGCs vs. normal

ipRGCs (b) comparison. Five terms among the top ten enriched terms in each cluster are shown at right. Red to blue Pearson Correlation scale indicates the degree to which mRNA expression is positively (dark red), negatively (dark blue) or not correlated with the expression of the respective lncRNA.

Supplementary Files

This is a list of supplementary files associated with this preprint. Click to download.

- Additionalfile1TableS1.pdf
- Additionalfile2TableS2.xlsx
- Additionalfile3TableS3.xlsx
- Additionalfile4TableS4.xlsx
- Additionalfile5TableS5.xlsx
- Additionalfile6TableS6.xlsx
- Additionalfile7TableS7.xlsx
- Additionalfile8SupplementaryFiguresS1S6.pdf